Study of hole kinetics in bismuth by means of transverse electron focusing

I. F. Sveklo and V. S. Tsoĭ

Institute of Solid State Physics, Russian Academy of Sciences
(Submitted 22 October 1992)
Zh. Eksp. Teor. Fiz. **103**, 1705–1722 (May 1993)

The focusing of holes in bismuth by a uniform magnetic field has been studied. The mean free path of the holes at $T=1.7$ K has been determined. The temperature dependence of this mean free path has been measured. This dependence is discussed on the basis of electron-phonon and electron-electron scattering. Intervalley surface scattering has been studied. The effect of the surface state (i.e., the effect of ion etching) on the probability for the specular reflection of normally incident holes and electrons has been studied for the bisector and trigonal planes of bismuth. The results indicate that there is a charge at the bismuth surface. This surface charge is responsible for the high probability for specular reflection of current carriers from the surface. The magnitude and sign of this charge depend on the crystallographic orientation of the surface and on several other, poorly controlled parameters, in particular, the properties of an adsorbed film and the surface-treatment method. A method has been developed for directly observing the effect of a field on the probability for specular reflection of electrons. A screening of effects of bismuth-surface roughness by an external field during the reflection of electrons from the surface has been observed.

INTRODUCTION

Ballistic effects due to the carriers of the hole part of the Fermi surface of bismuth are difficult to observe over a broad temperature range. For example, the first-order cyclotron-resonance lines of the holes fall in a region in which weakly damped magnetoplasma waves propagate, and they are completely masked by the much larger impedance oscillations caused by these waves.[1] For size effects, the short mean free path of the holes is the primary cause of the difficulties in observing holes. The mean free path of holes in bismuth at $T=1.7$ K is $l_h \simeq 50$ μm according to our measurements based on a focusing of electrons by a transverse magnetic field (as discussed below). It thus becomes necessary—in a study of the rf hole size effect, for example—to carry out the measurements at $T \leqslant 1$ K and to use samples of high structural quality. The reason is that at a working frequency $f \simeq 10$ MHz the small value of l_h requires samples with thicknesses on the order of the skin depth. As the working frequency is increased, the requirement of a quasisteady electromagnetic field is violated. The simultaneous presence of electrons having the same density with a mean free path $\geqslant 1$ mm adds another complication to efforts to observe hole size effects.

In the present study, electron focusing has been developed further as a method for studying the kinetic properties of current carriers with a short mean free path ($\leqslant 50$ μm). The capability of studying kinetic characteristics of carriers under these conditions distinguishes electron focusing in a favorable way from other size effects. These other effects require considerably larger samples and, correspondingly, considerably larger carrier mean free paths. There is an improvement in the resolution of electron focusing as a method for separately observing the focusing of carriers of different signs.

In connection with the observation of a focusing of holes in bismuth it has become possible to study the scattering of carriers with charges of opposite sign (electrons and holes) by a bismuth surface. It has also become possible to study electron-hole transitions in the course of scattering and to learn how these processes are affected by changes in the surface state. In semimetals and semiconductors, a screening of roughness features by the field of the surface charge (a near-surface band curvature) may become effective in the reflection of carriers from the surface.[2,3] If carriers of opposite sign are present, the band curvature clearly does not create a potential barrier for the carriers of one type, so they may reach the surface. A radical difference in the specular-reflection coefficients for electrons and holes may result; this effect has indeed been observed in antimony by electron focusing.[3] It opens up a possibility of using electron focusing to study the charge state of a surface.

The effect of an electric field on the probability for specular reflection of electrons and holes is a topic of particular interest. The electron wavelength and the screening radius are of the same order of magnitude, so the change in the probability for specular reflection by screening of roughness features is only a small one in the case of normal incidence on the surface and intravalley scattering. The effect of the field should be vastly greater on the intervalley scattering of electrons in bismuth, for the following reason. Bozhko *et al.*[4] have shown that intervalley scattering is the predominant mechanism for the suppression of intravalley scattering of electrons in bismuth. The efficiency of intervalley scattering in bismuth is determined by the roughness of atomic scale. Since the Debye screening length in bismuth is ~ 200 Å, i.e., much greater than interatomic distances, we would expect screening of the roughness of atomic scale by the surface-charge field to prevent inter-

 1063-7761/93/050839-10$10.00 © 1993 American Institute of Physics

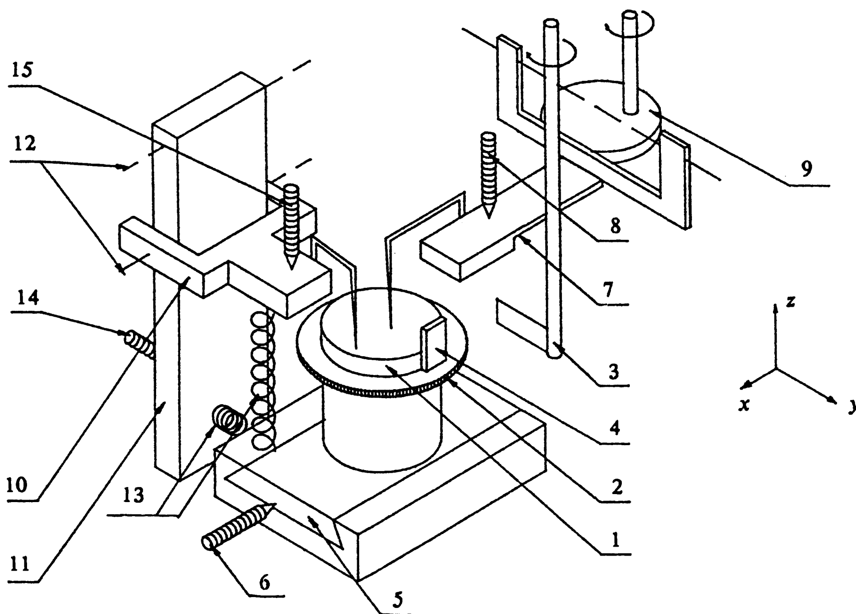

FIG. 1. Measurement head. *1*—Test sample; *2*—stage; *3*—pusher; *4*—mirror; *5*—platform; *6, 8, 14, 15*—screws; *7*—restoring spring; *9*—cam; *10, 11*—supports; *12*—needle supports; *13*—spring.

valley scattering and thereby cause a substantial increase in the probability for intravalley specular reflection.

EXPERIMENTAL APPARATUS AND PROCEDURE

The measurements were carried out by electron focusing[5] on bismuth samples grown in a dismountable polished quartz mold. The samples were disks 10 mm in diameter and 2 mm thick. The normal to the plane of the sample surface was parallel to either the $\mathbf{C}_2$ or the $\mathbf{C}_3$ axis.

The samples were synthesized from copper and tungsten wire 100 μm in diameter and sharpened by an electrochemical technique in a 10% KOH solution with a potential difference of a few volts across the electrodes.

The measurement head was a refinement of that of Ref. 6 and made possible the following manipulations at liquid-helium temperature: 1—independent adjustments of the contacts, i.e., of the collector and the emitter; 2—controllable adjustment of the collector-emitter distance L (to 30 μm); 3—plane-parallel displacement of a sample with respect to the measurement head; 4—controllable movement of the contacts, i.e., the collector and emitter, in mutually perpendicular directions; 5—change in the orientation of the sample with respect to the measurement head (rotation).

Figure 1 shows the basic parts of the measurement head. The sample, *1*, is mounted on a miniature stage *2*, which can be rotated around its own rotation axis by means of pusher *3*. The angular position of the sample is monitored by mirror *4* cemented to the stage. A laser beam is incident on the mirror. By monitoring the position of the reflected beam over a distance ~ 1 m, one can determine the angular position of the sample within less than 1°. In turn, stage *2* is mounted on a platform *5* which can be moved along the x axis by means of screw *6*. The emitter is attached to restoring spring *7*, whose position (and thus the position of the emitter) along the z direction is determined by the position of screw *8*. Its position along the x axis is determined by the position of cam *9*. By turning screw *8*, one can thus lift the emitter and place it on the surface of the sample. With the help of cam *9* one can move the emitter with respect to the measurement head along the x axis. Since the cam rotates without reducing gears, the step of the emitter movements along the x direction is ~ 10–20 μm. As a rule, this type of movement is used to change the distance between the collector and the emitter. The collector is attached to support *10*. Support *10* is mounted on support *11*, and support *11* is mounted on the body of the head, on needle bearings *12*. These bearing provide rotation around specified axes and prevent essentially any spontaneous movement. Springs *13* press supports *10* and *11* against screws *14* and *15* in such a way that by turning screw *14* one can move the collector along the y axis with respect to the sample, while by turning screw *15* one can raise the collector and place it on the surface of the sample. The screws are turned through reducing gears, so it is possible to achieve displacements of the microscopic contacts in steps of ~ 1 μm. The sharp points and the sample can be moved at liquid-helium temperature. The sample on the measurement head is immersed directly in liquid He^4. The distance between the collector and the emitter and the orientation of the line of contacts with respect to the crystallographic axes of the sample are monitored with the help of two BM-51-2 microscopes with a large focal length.

A particular effort was made to reduce the dimensions of a defective region of the sample when the contacts were brought close to each other. For this purpose, the measurements were carried out in two steps. First, the contacts (the collector and the emitter) were positioned in an initial region on the surface of the sample along the crystallographic direction of interest, at the desired distance. That position of the z-motion screws at which the contacts touched the surface of the test sample was determined. The contacts were then raised, the sample was moved 200–300

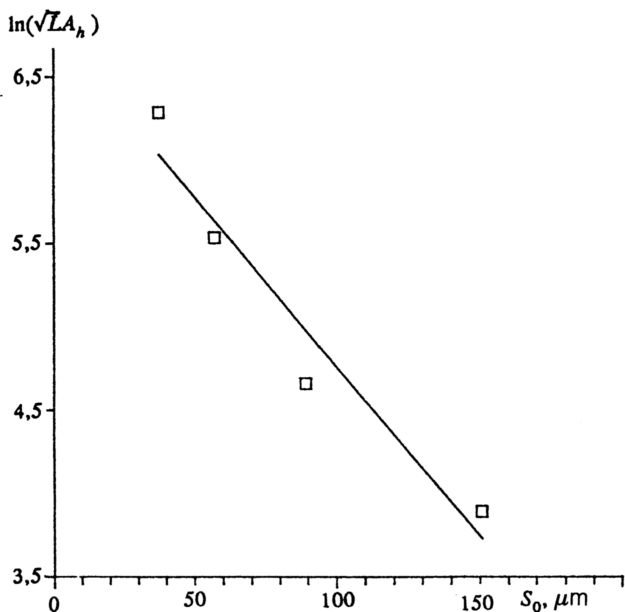

FIG. 2. Plot of $\ln(\sqrt{L}A_h)$ versus S_0 for various distances between the L contacts at $T=1.7$ K. The length of the electron trajectory, S_0, was calculated from $S_0=\pi L/2$.

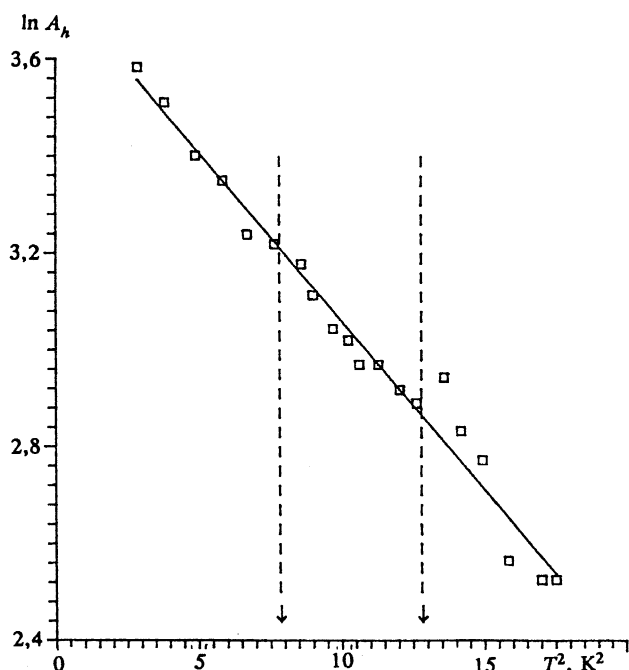

FIG. 3. Measured temperature dependence of the amplitude (A_h) of the hole electron-focusing line. The collector-emitter distance was $L=35$ µm.

µm, and the contacts were repositioned, in the same geometry, but on a different (high-quality) region of the surface. Only after the contact had been placed on the surface was a small potential applied to it ($\sim$4 V; the ballast resistance was $\sim$4 kΩ) to monitor the presence of the contact.

EXPERIMENTAL RESULTS

Measurements of the hole mean free path

The use of electron focusing to measure the carrier mean free path is based on the dependence of the amplitude A of the electron-focusing line on the carrier mean free path l. For a cylindrical Fermi surface this functional dependence is[7,8] $A \sim \sqrt{d/L}\exp[-S_0/l]$, where S_0 is the length of the electron trajectory from the emitter to the collector, d is the size of the contact, and L is the distance between contacts. The factor $\sqrt{d/L}$ incorporates the size of the region on the Fermi surface whose electrons are focused to the collector. It can be seen from this formula that by measuring the amplitude of the electron-focusing line for various distances L one can determine the absolute value of the carrier mean free path l, and by measuring the temperature dependence of A one can determine the temperature dependence of l.

The measurements of the hole mean free path were carried out on a sample whose $\mathbf{C}_2$ axis ran along the normal to the surface. The line of contacts was perpendicular to $\mathbf{C}_3$, and the magnetic field was perpendicular to the line of contacts. Because the amplitude of the hole line, A_h, is very sensitive to the temperature, measurements were carried out at the lowest temperature possible in our apparatus, $T=1.7$ K. Figure 2 shows the results of the measurements. The length of the trajectory of the holes was calculated from the formula $S_0=\pi L/2$. The distance between contacts, L, was determined from the position of the first hole electron-focusing line in the magnetic field. The apparent reason for the nonlinearity of the plot of $\ln(\sqrt{L}A_h)$ versus S_0 is a deviation of the line of contacts, **L**, from the normal to the major axis of the hole ellipse. This deviation could not be eliminated. At small distances between contacts ($\approx$30 µm), this deviation could have a significant effect on the value of A_h. As a result of the measurements (Fig. 2) we found the value $l_h \simeq 50$ µm for the hole mean free path.

The temperature dependence of the hole mean free path was measured for a collector-emitter distance $L=35$ µm. The results of the measurements of A_h over the temperature interval 1.7–4.2 K are shown as a plot of $\ln A_h(T^2)$ in Fig. 3. A least-squares fit of the experimental data by $\ln A_h = BT^N + C$, where B, N, and C are adjustable parameters, yields $N=2.01$, $B=-6.8 \cdot 10^{-2}$, and $C=3.37$ with a standard deviation of 7% (by way of comparison, the standard deviation with $N=3$ is 8.4%). The hole mean free path can thus be approximated by the function $l_h \approx \beta/T^2$, where $\beta=8.01 \cdot 10^{-2}$ cm·K^2. On all the $l(T)$ curves which we measured it was possible to observe local deviations from a smooth plot near temperatures of 2.8 and 3.6 K.

Probability for specular reflection

We studied the crystallographic anisotropy and the effect of the surface state on the values of q_e and q_h, i.e., the probabilities for specular reflection of respectively electrons and holes, in the case of normal incidence. We also studied the effect of an electric field on the probability of

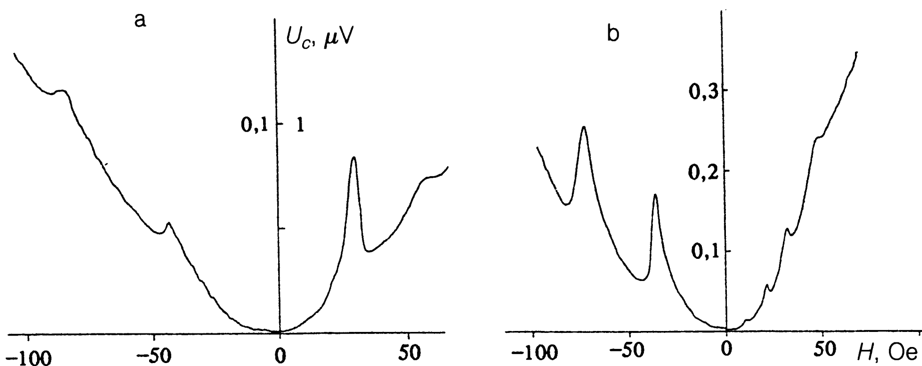

FIG. 4. Collector voltage U_c versus the magnetic field. The positive direction for the magnetic field corresponds to a focusing of electrons, and the negative direction to a focusing of holes. **n**|| $\mathbf{C}_2$. a—The line of contacts, **L**, is perpendicular to the major axis of the electron ellipsoid, with **H**, **L**=25°; b—**n**|| $\mathbf{C}_2$, **L**⊥ $\mathbf{C}_3$, **H**⊥ **L**.

specular reflection of electrons. In some of these experiments we used bismuth single crystals (grown in a polished quartz mold) whose surfaces were not subjected to any further processing. Other experiments were made with the same single crystals after their surfaces were etched by Ar^+ ions. The ion etching was carried out in a VUP-4 apparatus. The accelerating voltage was $\approx$600 eV, the argon pressure in the chamber was $\approx 10^{-3}$ torr, and the etching time was $\approx$1 min.

Figure 4 shows experimental results on U_c for a sample with an unetched surface in the configuration **n**|| $\mathbf{C}_2$, where **n** is the normal to the surface of the sample. The positive direction of the magnetic field corresponds to electron focusing, and the negative direction to hole focusing. An important point is that the measurements of the electron and hole focusing were carried out with the contacts in the same positions. In this case the electrons and holes are reflected from the same region on the surface of the sample. The data in Fig. 4a were obtained in a configuration in which the line of contacts **L** was perpendicular to the major axis of the electron ellipsoid, with **H**, **L**=25°. This angle between **H** and **L** was chosen empirically to maximize the amplitude of the "electron" electron-focusing line. The structure of the Fermi surface of bismuth is such that the geometry for observing the maximum electron line is not the same as that for observing the maximum hole line. Since the hole ellipsoid is stretched out considerably along the $\mathbf{C}_3$ axis, and since the major axes of the electron and hole ellipsoids make an angle $\approx$84° in the plane perpendicular to $\mathbf{C}_2$, the amplitude of the hole line is small in the specified orientation of the line of contacts with respect to the crystallographic axes of the sample, with **H**⊥ **L**. In the experimental geometry in Fig. 4b (**L**⊥ $\mathbf{C}_3$, **H**⊥ **L**) the amplitude of the hole line is at a maximum. Note the "oscillations" in $U_c(H)$ when the direction of the magnetic field corresponds to focusing of electrons. These oscillations, which are not periodic in the magnetic field, are very sensitive to the orientation of the line of contacts with respect to the crystallographic axes of the sample. When the magnetic field is rotated, some of the these oscillations shift up the field scale, and other disappear. Although we did not carry out a detailed study of these oscillations, there are indications that they result from a focusing of electrons of noncentral cross sections of the three electron ellipsoids of the bismuth Fermi surface.

It was also possible to observe a focusing of holes in a sample with **n**|| $\mathbf{C}_3$ (Fig. 5; the surface of the sample had not been subjected to ion etching). In this case, the line of contacts was put in the orientation **L**⊥ $\mathbf{C}_1$ in order to retain the capability of observing a focusing of electrons when the magnetic field was reversed. The amplitude of the hole line in this experimental geometry turned out to be very sensitive to the orientation of the contacts with respect to the crystallographic axes of the sample. The probable reason is that the amplitude of the hole line is substantially affected by even a small deviation of the major axis of the hole ellipsoid from the $\mathbf{C}_3$ direction. Working from the extreme dimensions of the electron and hole ellipsoids of the Fermi surface, we found that the ratio of the fields at which hole focusing and electron focusing are observed was 6.6. The experimental value is 6.3 ± 0.7 [averaged over various experimental $U_c(H)$ curves corresponding to various positions of the contacts]. This result implies, in particular, a deviation of **n** from the $\mathbf{C}_3$ direction.

From the amplitudes of the first and second lines of the electron focusing of electrons and holes we determined the probability q during reflection from the surface for two orientations of this surface. The samples were then subjected to ion etching, and the procedure was repeated for

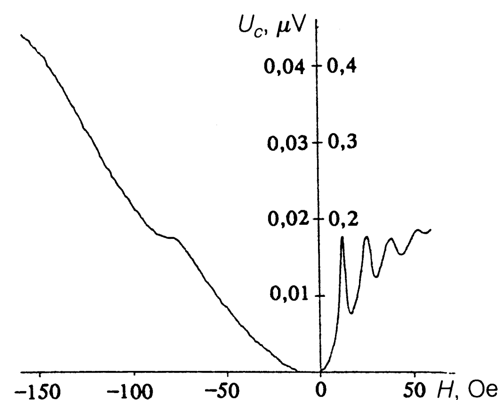

FIG. 5. Collector voltage U_c versus the magnetic field. The positive direction of the magnetic field corresponds to a focusing of electrons, a negative direction to a focusing of holes. **n**|| $\mathbf{C}_3$. The line of contacts **L** is perpendicular to the major axis of the electron ellipsoid, **H**⊥ **L**.

TABLE I. Coefficients of the specular reflection of electrons and holes for various crystallographic orientations of the surface of the bismuth sample.

	$\mathbf{n} \parallel C_2$		$\mathbf{n} \parallel C_3$	
	Before ion etching	After ion etching	Before ion etching	After ion etching
Electrons	0,22 ± 0,09	0,31 ± 0,07	0,71 ± 0,09	0,24 ± 0,03
Holes	0,94 ± 0,06	0,42 ± 0,2	0,57 ± 0,1	0,4 ± 0,1

the etched surfaces. The results of these measurements are shown in Table I.

To observe the effect of an electric field on the probability for specular reflection of electrons, we used samples with $\mathbf{n} \parallel C_3$ whose surfaces had been etched with Ar^+ ions. The ion etching caused a dramatic increase in the probability for intervalley electron-electron scattering upon reflection from the surface. This circumstance made it easier to detect the minimal decrease in intervalley scattering upon a screening of the roughness features by the field of the surface charge. To create an external electric field normal to the plane of the sample, a capacitor was fabricated on the surface of the sample (Fig. 6). One plate of the capacitor was the sample itself; the other was an aluminum film deposited on an insulating spacer. A thin layer of insulator, *2*, was deposited on the sample surface *3*. Several rectangular apertures 0.1×1 mm^2 in size were then formed in the insulator by photolithography. A thin film of aluminum, *1*, was then deposited through this mask. The aluminum film, of course, made electrical contact with the sample. To eliminate this contact, a static voltage ≈ 10 V was applied to the film with respect to the sample. A fairly high current passed in regions in which the film and sample were in electrical contact, and the aluminum film "burned up" along the boundaries of the apertures in the insulator. The electrical contact between the film and the sample was thus eliminated. A potential contact was applied to the aluminum film with conducting cement. The stability of this contact was monitored by measuring the film-sample capacitance. The typical value of this capacitance was ≈ 200 pF. As the insulator we used silicon monoxide, SiO, or FP-383 photoresist. The SiO was deposited on the surface of the sample by vacuum deposition. Its typical thickness was ~ 5000 Å. The photoresist was deposited on the surface of the sample by a centrifuge. It thickness was $\approx 1 \mu$m. The thickness of the insulator was found from the capacitance of the capacitor and also with the help of an MII-7 interference microscope.

The collector and the emitter were placed in neighboring apertures in the insulator (Fig. 6b), and a $U_c(H)$ curve was measured without an electric field in the capacitor and then with an applied electric field, close to the breakdown value for the given insulator. When we used SiO as the insulator we were not able to find changes in $U_c(H)$ when the electric field was applied. After the deposition of a SiO film, the probability for specular reflection of electrons increased to a level 0.1–0.15 higher than that of a control region of the surface of the sample. When a SiO film was deposited on a sample with $\mathbf{n} \parallel C_2$ the specular-reflection probability decreased from 0.25 (for a region of clean surface) to 0.08 (for the region under the SiO film). When we used the FP-383 photoresist as insulator, we were able to observe changes in $U_c(H)$ when a voltage was applied to the capacitor. Figure 7 shows experimental curves of $U_c(H)$; the light line corresponds to a zero voltage, and the heavy line to the application of a voltage of -30 V. The electric field at the surface for this voltage is $\approx 6 \cdot 10^5$ V/cm. The application of a voltage at the opposite polarity

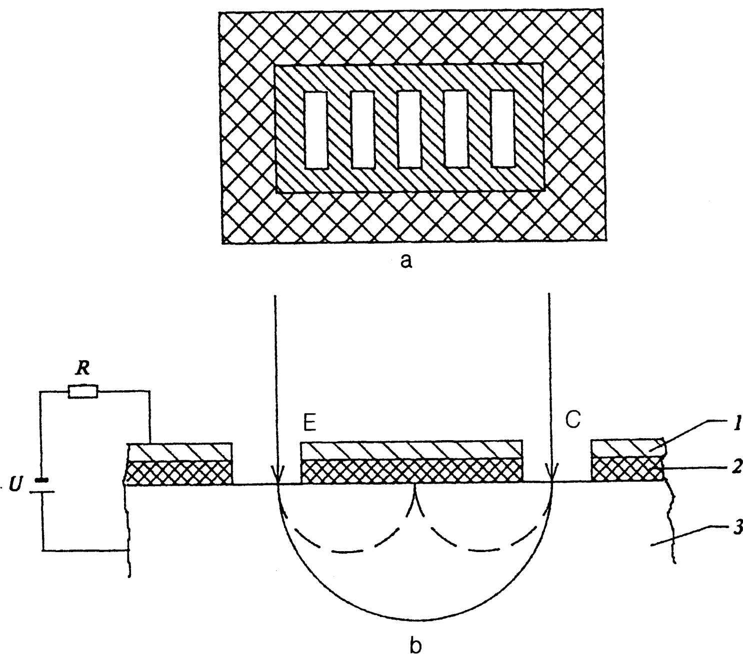

FIG. 6. Experimental layout for observing the effect of an external electric field on the nature of the reflection of conduction electrons from the surface of a sample. The hatching shows the deposited aluminum film. The cross hatching shows the insulating film. For clarity, parts of panels a and b are shown in different scales. a: Top view of the surface. b. Sectional view of the capacitor which was formed. *E*—Emitter; *C*—collector; *1*—aluminum film; *2*—insulating film; *3*—test sample; *U*—voltage source; *R*—ballast resistance. Two trajectories, of electrons which form the electron-focusing line without reflection from the surface and after a single reflection from the surface (the dashed line), are shown.

FIG. 7. Curves of $U_c(H)$ recorded at a zero voltage across the capacitor (light line) and at a voltage of -30 V (heavy line).

had no effect on the shape of the $U_c(H)$ curves. The most important change in $U_c(H)$ is the appearance of a third electron-focusing line after the application of the voltage. In the absence of the voltage this line is not resolved. The application of the voltage had essentially no effect on the amplitude of the second line.

Curiously, after a sample (with $\mathbf{n} \| \mathbf{C}_3$) coated with a photoresist film was stored at room temperature for ~ 2 weeks, the change in the $U_c(H)$ curve upon the application of an electric field disappeared. If the photoresist was subjected to a standard "tanning" at 120 °C, the probability for specular reflection of electrons from the resist-covered surface increased substantially, to ~ 0.8. After this event, no effect of the field was observed.

DISCUSSION

The temperature dependence of the electron mean free path l_e in bismuth has been measured several times previously, by various methods: the rf size effect,[9] cyclotron resonance,[10,11] and electron focusing.[12] These measurements have yielded a dependence $l_e = \beta/T^2$, where $\beta = 1$–1.5 cm·K^2, in the temperature interval 1.5–4.2 K. This dependence is characteristic of electron-electron scattering. However, since the electron ellipsoid of the bismuth Fermi surface is highly elongated, the electron-phonon interaction should also give rise to a dependence $l_e \propto 1/T^2$ in the temperature interval in which the conditions $p_1 > \hbar q_{\text{ph}} > p_2$, p_3 hold ($\hbar q_{\text{ph}}$ is the momentum of a phonon of energy $k_B T$, and p_1, p_2, and p_3 are the dimensions of the electron ellipsoid).[9] Since there have been no previous measurements of the temperature dependence of the mean free path of the holes in bismuth, there has been no discussion of whether the holes are scattered by phonons or by holes.

To calculate the probability W for a scattering of holes by phonons we calculate the strain potential Λ for an isotropic model, ignoring the crystallographic anisotropy of the phonon dispersion curves, for a Fermi surface consisting of an ellipsoid of revolution with a dispersion $\varepsilon(\mathbf{k})$:

$$\varepsilon(\mathbf{k}) = \hbar^2/(2m_1)(k_x^2 + k_y^2) + \hbar^2/(2m_2)k_z^2, \quad (1)$$

where m_1 and m_2 are the effective masses of electrons along

the principal axes of the ellipsoid. Since a focusing of holes of the central cross section of the Fermi surface is observed experimentally, we examine the scattering probability for a hole with a wave vector $\mathbf{k}=(k_F,0,0)$. After some lengthy manipulations, we find

$$W=\frac{4}{\pi^2}\frac{\Lambda^2}{\rho s}\frac{k_F^3}{\hbar v_F}\left(\frac{T_Q}{T}\right)\int_0^{\pi/2}d\theta\int_0^{\pi/2}\frac{d\varphi}{\cos\varphi}\times Q^4\frac{\exp(QT_Q/T)}{[1-\exp(QT_Q/T)]^2}, \qquad (2)$$

where

$$T_Q=2k_F\hbar s,\quad Q=\frac{\sin\theta\cos\varphi}{m_1/m_2+(1-m_1/m_2)\sin^2\theta},$$

s is the sound velocity in bismuth, ρ is the density of bismuth, and v_F is the hole Fermi velocity.

From Eq. (1) we find

$$\ln A_h=\text{const}-S_0/v_FW, \qquad (3)$$

where $S_0=\pi L/2$ is the trajectory length. Figure 8 shows results calculated on the temperature dependence of the amplitude of the electron-focusing line for holes ($L=35$ μm, $\Lambda=1.1$ eV, $k_F=1.4\cdot10^6$ cm^{-1}, $\rho=9.8$ g/cm^3, $s=2\cdot10^5$ cm/s, $v_F=8\cdot10^7$ cm/s, and[1)] $m_1/m_2=0.15$). As expected, the temperature dependence of $\ln A_h$ is not quadratic in the interval 1.7–4.2 K. A least-squares fit of $\ln A_h=BT^N+C$ (B, N, and C are adjustable parameters) to the results of these calculations yields $N=1.16$ with a standard deviation of 3.6% (by way of comparison, the standard deviation with $N=2$ is 32%). An $l_h=\beta/T^2$ approximation yields $\beta\approx40$ cm $\cdot$ K^2. This large deviation from the experimental value of β suggests that the hole mean free path in bismuth is not governed by scattering by phonons.

Let us now estimate the probability for the scattering of holes by holes. Taking the scattering of carriers by each other in bismuth to be a scattering by a screened Coulomb potential (with a screening length λ_s), we can use the following expression to estimate the mean free path:[13]

$$l_{hh}=\tau v_F\simeq v_F\frac{2\hbar^3\varkappa^2}{me^4}\left(\frac{\varepsilon_F}{k_BT}\right)^2\frac{1}{\Phi_0(x)}\frac{2\xi^2}{H_+(\xi)}, \qquad (4)$$

where

$$\Phi_0(x)=\pi^2/2[1+(x/\pi)^2],$$

$$x=(\varepsilon_k-\varepsilon_F)/T\approx0;$$

$H_+(\xi)$ is the screening function

$$H_+(\xi)=\frac{1}{16\pi}\left[\frac{1}{\xi}\operatorname{arctg}\frac{1}{\xi}+\frac{1}{1+\xi^2}\right],$$

$\xi=1/2k\lambda_s$, $\varkappa\approx100$ is the dielectric constant, m is the effective carrier mass, and τ is the relaxation time. The screening length λ_s for bismuth was calculated in Ref. 14; it is equal in order of magnitude to the Debye length $R_D\approx2\cdot10^{-6}$ cm. We thus find $l_{hh}\approx5.5/T$ cm $\cdot$ K from (4). This value is again at odds with the experimental value in order of magnitude.

The screening length λ plays an important role in a calculation of the probability for electron-electron scattering. In addition to the screening by carriers (electrons and holes) there may be a screening by phonons. The best known manifestation of this screening is superconductivity, in which case the screening effect is so strong that the Coulomb repulsion of electrons gives way to an attraction. For normal metals, the incorporation of electron scattering accompanied by the creation and absorption of virtual phonons may lead to a substantial change in the electron-electron scattering probability. For example, the temperature dependence of the resistance, $\rho(T)$, was measured for aluminum single crystals in Ref. 15. A dependence $\rho(T)=A_\rho T^2$ was found, where $A_\rho=2.8\cdot10^{-15}$ Ω/μC^{-2}. This figure is considerably larger than the theoretical value $A_\rho=0.12\cdot10^{-15}$ Ω/μC^2 which was found in Ref. 16 for electron-electron scattering without an interaction through virtual phonons. A calculation was carried out on electron-electron scattering for aluminum involving virtual phonons in Ref. 17. The value found for the coefficient A_ρ agrees with the measurements of Ref. 15. Later, in Ref. 18, a calculation was carried out on electron-electron scattering for alkali metals, with allowance for electron-electron scattering with and without the involvement of virtual phonons. Significantly, the participation of virtual phonons in the electron-electron scattering increases the scattering probability by an order of magnitude.

In summary, we do not have a satisfactory theoretical description of the observed temperature dependence of the hole mean free path. In bismuth the momentum of a longitudinal phonon is comparable to the Fermi momentum of holes along the $\mathbf{C}_2$ and $\mathbf{C}_3$ directions at temperatures of 2.81 and 7.18 K, respectively.[19] For a given local group of holes of the bismuth Fermi surface which form the electron-focusing line in the experiments, a calculation of the mean free path based on the scattering of holes by holes involving virtual phonons leads to a better agreement with experiment. It explains the appearance of structural features on the temperature dependence of the hole mean free path at 2.8 and 3.6 K.

Analyzing the data in Table I on the measured probabilities for specular reflection of electrons and holes, we draw the following conclusions. Since the de Broglie wavelengths of electrons and holes are roughly the same, it follows from the difference in the specular-reflection probabilities for electrons and holes that there is a fairly large positive charge on the surface perpendicular to the $\mathbf{C}_2$ direction. During ion etching, a large number of defects arise on the surface, reducing the surface charge and increasing the surface roughness. These conclusions are indicated by the significant decrease in the coefficient for specular reflection of holes and some increase in that for electrons after the ion etching. We can estimate a lower bound on the surface-charge density for $\mathbf{n}\|\ \mathbf{C}_2$ by again postulating that a positive surface charge leads to a curvature of the bands near the surface of the sample, by an amount greater

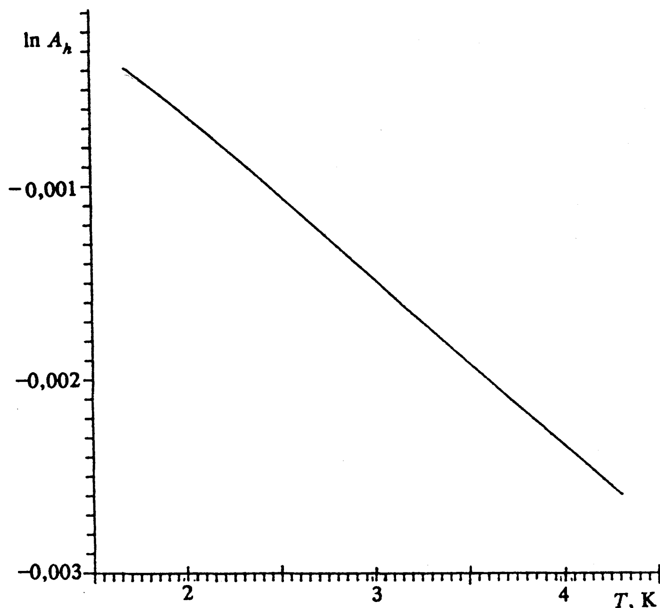

FIG. 8. Calculated temperature dependence of the amplitude of the electron focusing of holes determined by the scattering of holes by phonons. The distance between contacts is $L=35$ μm.

than ε_{Fh}, where ε_{Fh} is the hole Fermi energy (equivalently, $\sim 10^{12}$ electrons/cm^2).

At a bismuth surface with $\mathbf{n}\|$ C_3 there is a negative charge. Its magnitude is probably lower than that at the face with $\mathbf{n}\|$ C_2 (the difference between the specular-reflection coefficients for electrons and holes is not this great). Ion etching of the surface also leads to an increase in the surface roughness and a decrease in the charge. In terms of the sign of the surface charge, this situation is similar to that an antimony surface with $\mathbf{n}\|$ C_3 (Ref. 3).

The minimum probability for specular reflection of electrons is far smaller than that for holes. The reason is that the main cause of the decrease in the specular-reflection coefficient of electrons is intervalley scattering.[4] The probability for an electron-hole transition is low,[20] so holes can be scattered only in intravalley processes. As a result, the specular-reflection coefficient for holes is high even in the case of an etched surface.

The electron part of the bismuth Fermi surface consists of three highly elongated ellipsoids, which are sent into each other by a rotation of 120° around the C_3 axis (Fig. 9). The surfaces of these ellipsoids are approximately cylindrical, so essentially all the electrons coming from the emitter move in planes perpendicular to the major semi-axes of the ellipsoids. In the case $\mathbf{H}\|$ C_1, the Larmor radius of electrons moving either along or parallel to EC is half that of the electrons moving at an angle 60° to this direction (Fig. 9). The projections of the electron trajectories onto the plane of the sample are shown by the straight lines in Fig. 9. At points *1–6* and C, electrons are focused and reflected from the surface. The arrows show possible directions of the motion after reflection. In the case of intervalley scattering at the surface, the plane of motion of the electron changes, so there is the possibility that electrons from all three valleys will reach the collector.[8] The amplitude of the electron-focusing line in the experimental geometry used is determined by both intravalley and intervalley scattering in this case. The circles and plus signs are points which an electron reaches after intervalley and intravalley reflection, respectively. At a

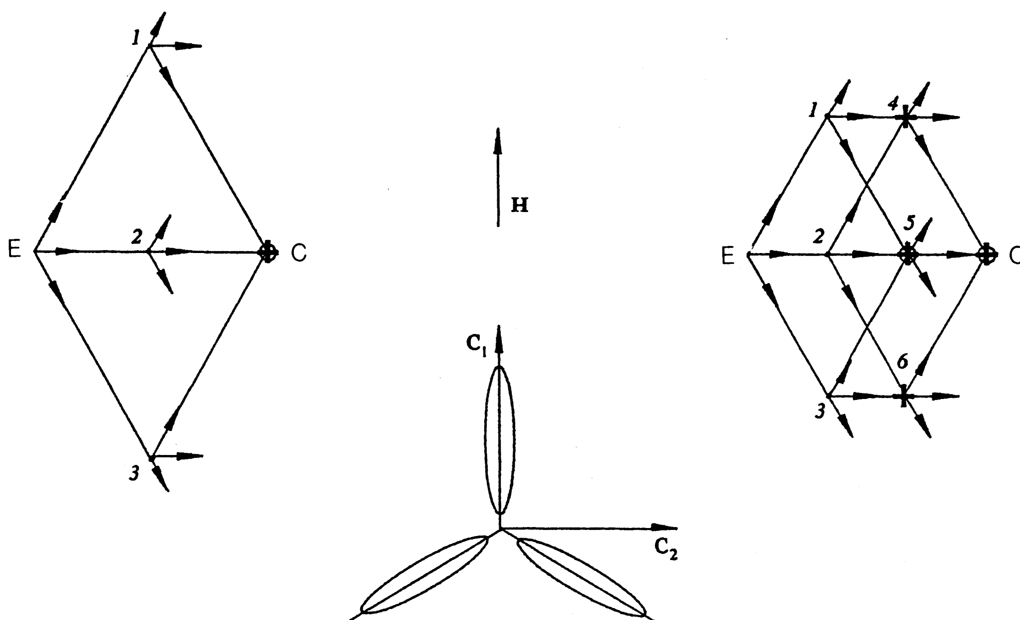

FIG. 9. Projections onto the plane of the sample of electron valleys (ellipsoids) of bismuth and of trajectories of electrons which form the second electron-focusing line (at the left) and the third line (at the right).

point without these symbols the electrons are focused without reflection from the surface. The amplitude of the electron-focusing line is determined by the sum of the various possible trajectories (e.g., E14C) along which an electron from the emitter reaches the collector for the various types of surface scattering.

The nature of intervalley scattering in this geometry was studied in Refs. 21 and 4. In the case of a single-valley electron spectrum, the change in the amplitude of the nth line upon a change Δq is $\Delta A_n \approx A_1(n-1)q^{n-2}\Delta q$. In other words, the change in A_n decreases with increasing n, because of the relation $q<1$. In the case of a multivalley spectrum the result is $A_2 = A_1 q_e + 2A_1 \alpha q_e^{\text{int}}$, $A_3 = A_1 q_e^2 + 6A_1\alpha^2(q_e^{\text{int}})^2$, where the coefficient α is determined by the experimental geometry, including the dimensions of the contacts, the structure of the Fermi surface, and the nature of the intervalley scattering (random or correlated). The quantity q_e^{int} is the probability for intervalley electron-electron scattering. Intervalley electron-hole scattering has a low probability[20] and has been ignored.

Since we have $q_e + 2q_e^{\text{int}} = 1(\Delta q_e = -2\Delta q_e^{\text{int}})$, a decrease in q_e means an increase in q_e^{int}, and vice versa. At a small value of Δq, with equiprobable scattering in all the electron valleys, we have $\Delta A_2 = A_1\Delta q_e(1-\beta)$ and $\Delta A_3 = 2A_1 q_e \Delta q_e(1-3\alpha^2)$. We recall that electron focusing should be observed in even fields in the case of diffuse reflection also,[8] since the probability density for an electron to reach the mirror state is not zero. In bismuth, with a reflection which is initially totally diffuse (in particular, the probabilities for reflection into all the electron valleys are equal), we have $\alpha = 1$, and no changes should occur in A_2 even if intervalley scattering is completely suppressed. The explanation is as follows (Fig. 3). When the second electron-focusing line forms (at the left in Fig. 3) the electrons which have been emitted from the emitter and which are moving toward the collector initially focus at point *2*. This flux then splits into three equal fluxes as a result of intervalley scattering; the three are directed as indicated by the arrows. Only 1/3 of the electrons focused at point *2* contribute to the amplitude of the second line. However, 1/3 of the flux comes from each of the two other valleys. After the electrons of these valleys leave the emitter, they are focused at points *1* and *3*, respectively, in Fig. 9. After the intervalley scattering they are focused on the collector. If intervalley scattering is excluded, the electron-focusing line is formed exclusively by the electrons of one valley, and the entire flux moves toward the collector, after reflection at point 0, and contributes to the line amplitude. If intervalley scattering is excluded, there are accordingly no changes in the flux forming the second electron-focusing line. Similar arguments show that a change should occur in the amplitude of the third line (at the right in Fig. 3) at the same time, and this change should furthermore have the sign opposite that in the case of a single-valley electron spectrum.

Earlier studies[4] of the reflection of electrons from a bismuth surface showed that a totally diffuse reflection of electrons occurs if the surface has been subjected to ion etching. As we mentioned earlier, the surfaces of the samples were initially charged. The magnitude of this charge was so great that is led to differences in the nature of the reflection of electrons and holes. The manifestation of the field effect under these conditions was discussed above; it should be as follows: 1. The effect depends on the polarity of the field. 2. The field does not affect the amplitude of the second electron-focusing line. 3. The decrease in the probability for intravalley reflection due to the field effect leads to an increase in the amplitude of the third electron-focusing line, and vice versa. This is the behavior which is observed experimentally. The low probability for specular reflection makes it impossible to observe changes in the amplitudes of lines of higher indices. If the valleys are nonequivalent because of differences in the valleys themselves or, possibly, because of the orientation of the normal to the surface with respect to the crystallographic axes of a sample, the magnitude of the field effect and also its sign will be determined by the value of α.

Working from the experimental data, we can estimate the change in the probability for specular reflection upon the application of an electric field: $\Delta q_e \approx -2\Delta q_e^{\text{int}} \sim 0.1$.

When insulating films are deposited on the bismuth surface, an additional charge arises at the bismuth-insulator interface. The magnitude of this charge is determined by the nature of the used insulator and also by the surface structure of the sample. Furthermore, during vacuum deposition of insulators the structural defects at the surface may undergo a relaxation because of the low melting point of bismuth. We were unable to find an insulator which did not give rise to an additional surface charge; this circumstance is probably the reason for the very weak field effect.

Generalizing the results, we can conclude that the nature of the reflection of current carriers from a surface in bismuth is determined primarily by the electronic state of the surface, i.e., by the presence of surface charge. This charge may be either negative or positive. Ion etching of the surface leads to a decrease in the surface charge. When films are deposited on the surface, the magnitude of the surface charge may increase. What remains unclear is the nature of the surface charge: Is this a property of an atomically clean surface, or is it a manifestation of an adsorption of impurities on the surface? Resolving this question will require further study, with a controlled surface state—in ultrahigh vacuum.

[1)]For holes in bismuth, the true value of this ratio is $m_1/m_2=0.09$. Since the T_Q dependence in the integrand in (2) is in the form of the expression QT_Q/T, we hoped to compensate for the anisotropy of the sound velocity s in bismuth by increasing m_1/m_2.

[1]S. M. Cheremisin, *Candidate's Dissertation*, Inst. Phys. Prob., Moscow, 1973.

[2]V. Ya. Kravchenko and É. I. Rashba, Zh. Eksp. Teor. Fiz. **56**, 1713 (1969) [Sov. Phys. JETP **29**, 918 (1969)].

[3]V. S. Tsoĭ and I. I. Razgonov, Pis'ma Zh. Eksp. Teor. Fiz. **23**, 107 (1976) [JETP Lett. **23**, 92 (1976)].

[4]S. I. Bozhko, I. F. Sveklo, and V. S. Tsoĭ, Fiz. Nizk. Temp. **15**, 710 (1989) [Sov. J. Low Temp. Phys. **15**, 397 (1989)].

[5]V. S. Tsoĭ, Pis'ma Zh. Eksp. Teor. Fiz. **19**, 114 (1974) [JETP Lett. **19**, 70 (1974)].

[6] V. S. Tsoĭ, N. P. Tsoĭ, and S. E. Yakovlev, Zh. Eksp. Teor. Fiz. **95**, 921 (1989) [Sov. Phys. JETP **68**, 530 (1989)].
[7] V. S. Tsoĭ and N. P. Tsoĭ, Zh. Eksp. Teor. Fiz. **73**, 289 (1977) [Sov. Phys. JETP **46**, 150 (1977)].
[8] V. S. Tsoĭ and Yu. A. Kolesnichenko, Zh. Eksp. Teor. Fiz. **78**, 2041 (1980) [Sov. Phys. JETP **51**, 1027 (1980)].
[9] V. F. Gantmakher and Yu. S. Leonov, Pis'ma Zh. Eksp. Teor. Fiz. **8**, 264 (1968) [JETP Lett. **8**, 162 (1968)].
[10] V. S. Édel'man and S. M. Cheremisin, Pis'ma Zh. Eksp. Teor. Fiz. **11**, 373 (1970) [JETP Lett. **11**, 250 (1970)].
[11] S. M. Cheremisin, V. S. Édel'man, and M. S. Khaĭkin, Zh. Eksp. Teor. Fiz. **61**, 1112 (1970) [Sov. Phys. JETP **34**, 594 (1971)].
[12] V. S. Tsoĭ, *Doctoral Dissertation*, Inst. Solid-State Phys., Cheronogolovka, 1978.
[13] V. F. Gantmakher and I. B. Levinson, *Scattering of Current Carriers in Metals and Semiconductors* [in Russian], Nauka, Moscow, 1984.
[14] D. H. Brownell, Jr., and E. H. Hygh, Phys. Rev. **164**, 909 (1967).
[15] J. H. J. M. Ribot, J. Bass, H. van Kempen, and P. Wyder, J. Phys. F **9**, L117 (1979).
[16] W. E. Lawrence and J. W. Wilkins, Phys. Rev. B **7**, 2317 (1973).
[17] A. H. MacDonald, Phys. Rev. Lett. **44**, 489 (1980).
[18] A. H. MacDonald, R. Taylor, and D. J. W. Geldart, Phys. Rev. B **23**, 2718 (1981).
[19] Y. Eckstein, A. W. Lawson, and D. H. Reneker, J. Appl. Phys. **31**, 1534 (1960).
[20] I. F. Sveklo and V. S. Tsoĭ, Pis'ma Zh. Eksp. Teor. Fiz. **49**, 290 (1989) [JETP Lett. **49**, 331 (1989)].
[21] V. V. Andrievskiĭ, E. I. Ass, and Yu. F. Komnik, Fiz. Nizk. Temp. **11**, 1148 (1985) [Sov. J. Low Temp. Phys. **11**, 631 (1985)].

Translated by D. Parsons